

Size Effect on the Physical Properties of CdS Thin Films Prepared by Integrated Physical-Chemical Approach

R. Sathyamoorthy^{1,*}, P. Sudhagar¹, S. Chandramohan¹, and U. Pal²

¹PG and Research Department of Physics, Kongunadu Arts and Science College, Coimbatore 641029, India

²Instituto de Fisica, Universidad Autonoma de Puebla, Apdo, Postal J-48, Puebla, México

Using an integrated physical-chemical approach, nanocrystalline cadmium sulfide (CdS) thin films were prepared by evaporating chemically synthesized CdS nanorods. Both the CdS nanorods and nanocrystalline thin films exhibited hexagonal wurtzite structure. Chemically synthesized CdS nanorods of about 7 nm average diameter were flexible, frequently folded to have elliptical cage linked chain structures and aggregate to form nanorod bundles. The bandgap energy of the nanocrystalline CdS films suffered a blue shift of about 0.07 eV due to intermediate quantum confinement of charge carriers. The reaction atmosphere was found to have strong effects on the particle size control of the nanostructures. Room temperature photoluminescence (PL) spectra of the films revealed a broad emission at about 429 nm related to recombination of excitons and shallowly trapped electron-hole pairs, along with the near-band-edge emission. Influence of particle size and defects on the structural and optical properties of CdS nanorods and nanocrystalline thin films are discussed.

Keywords: CdS Nanorod, Surfactant Assisted Synthesis, Thermal Evaporation, Quantum Confinement, Raman and Photoluminescence Spectroscopy.

1. INTRODUCTION

Semiconductor nanocrystalline thin films have attracted much attention in recent years in both fundamental research and technological applications, because of their tunable size dependent electronic and optical properties. For the past few decades, the synthesis of low-dimensional semiconductor materials with controlled morphologies like quantum dot, nanorod, nanowire, etc. have been motivated by their efficient applications in optoelectronics, biotechnology, catalysis, etc.^{1–3} Cadmium sulfide (CdS) nanostructures have been found to play an important role in optoelectronic devices such as laser light-emitting diodes.⁴ Different techniques have been employed to synthesize nanostructures, which include surfactant or template assisted,⁵ vapor-liquid-solid (VLS),⁶ colloidal micellar,⁷ and electrochemical process. Among them, the surfactant-assisted synthesis provides a good control over the synthesis parameters at ambient conditions. The non-ionic surfactant Triton 100-X (Polyoxyethylene tert-octylphenyl ether) is one of the suitable candidates among the surfactant family for CdS nanorod synthesis in controlled manner. Synthesis of CdS nanorods and nanowires using Triton 100-X as surfactant have been

reported by several groups.^{6–8} Synthesis of nanostructured thin films is a challenging task in recent years and this is overcome by preparing the nanomaterials by conventional chemical routes which are easy to scale up and subsequently depositing by physical methods.^{9–11} Limited reports are available for synthesizing nanostructured CdS thin films by vacuum evaporation. This paper reports the preparation of nanocrystalline CdS thin films by integrated physical and chemical approach, and demonstrates the dependence of particle size and defects on the structural and optical properties of CdS nanocrystalline thin films.

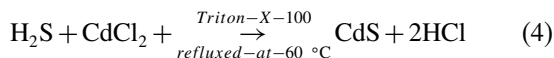
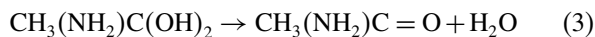
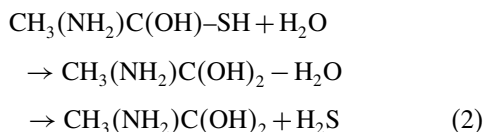
2. EXPERIMENTAL DETAILS

2.1. Synthesis of CdS Nanorods

The CdS nanorods were synthesized by organometallic-surfactant assisted method. In a typical synthesis of nanorods, a suspension consisting of cadmium oxide (CdO, 50 mmol) in 20 ml of Triton 100-X (~24 mmol) was prepared. Aqueous solution of thioacetamide in basic medium was added drop by drop to the above suspension under constant stirring at 60 °C in argon atmosphere. The resulting mixture was refluxed for 12 hours and left overnight. A possible reaction mechanism, similar

*Author to whom correspondence should be addressed.

to the one proposed by Zhu et al.,¹² in synthesizing CdS nanoparticles, is given below:



Equation (1) represents that the H_2O reacts with CH_3CSNH_2 to form $\text{CH}_3(\text{NH}_2)\text{C}(\text{OH})\text{-SH}$ by refluxing at 60°C . Repeating this process results in the formation of $\text{CH}_3(\text{NH}_2)\text{C}(\text{OH})_2$ and H_2S . Subsequently, $\text{CH}_3(\text{NH}_2)\text{C}(\text{OH})_2$ loses water to form CH_3CONH_2 (Eq. (3)). Further, the generated H_2S reacts with CdCl_2 to form CdS particles, whose surfaces are modified by the surfactant (Triton X 100). In order to remove the surfactant, the product was washed repeatedly with cyclohexane and diethyl ether and then dried.

2.2. Preparation of CdS Nanocrystalline Thin Films

CdS nanorods obtained by surfactant-assisted method were thermally evaporated on to pre-cleaned glass substrate using 12" HindHivac vacuum coater. Films were deposited at a constant rate of evaporation ($0.3 \text{ \AA}/\text{Sec}$) under a pressure of 10^{-5} Torr. The substrates were rotated by a rotary drive during the evaporation in order to obtain uniform film thickness. A quartz crystal monitor was used to monitor the thickness of the films. Thin films of about 630 \AA were prepared.

The structure of CdS nanorods and nanocrystalline thin films was studied using a Bruker AXS D8 X-ray diffractometer with $\text{CuK}\alpha$ radiation ($\lambda = 1.5406 \text{ \AA}$). Surface morphology and composition of the CdS nanorods were studied by transmission electron microscopy (TEM) analysis using a JEOL JSM-6360 electron microscope, with analytical system attached. The surface topography of the films was examined by atomic force microscopy (AFM) using a Nanoscope IIIa (Digital instruments) operated in tapping mode and oxide-etched pyramidal Si_3N_4 probe as tip. Optical absorption spectra were recorded for both CdS nanorod and nanocrystalline thin films by a JASCO V570 UV-Vis-NIR spectrophotometer. Raman spectra of the CdS nanorod samples, synthesized at different reaction atmospheres, were measured by a RENISHAW MICRO RAMAN 1000 spectrometer using He-Ne (632.8 nm) laser source at room temperature. Photoluminescence emission in the wavelength range of $400\text{--}600 \text{ nm}$ was recorded for CdS nanocrystalline thin films using a 488 nm line from an Ar^+ laser as the excitation source.

3. RESULTS AND DISCUSSION

3.1. Effect of Particle Size

The XRD patterns of CdS nanorods and thin films are shown in Figure 1. The observed reflections from CdS nanorods such as (002), (110) and (112) planes confirm the hexagonal wurtzite phase of CdS with lattice constants close to the bulk (JCPDS-41-1049). Bulk CdS usually exhibits cubic phase at room temperature and rarely exhibits the hexagonal phase.^{1,2} However, in the present work, the films prepared at room temperature exhibit hexagonal phase similar to the results obtained by Oliva et al.^{13,14} for their CdS thin films prepared by close space sublimation (CSS) technique.

In our CdS films, higher intensity of the (002) peak is due to a preferred orientation of crystallites along this direction. The mean crystallite size D , of the nanorods and films was calculated by the Scherrer formula:

$$D = \frac{K\lambda}{\beta \cos \theta} \quad (5)$$

where K is the shape factor, λ is the X-ray wavelength and β is the full width at half maximum (FWHM) of the diffraction peak on the 2θ scale. The crystallite size of the CdS nanorods and thin films is given in Table I. The particle size of CdS nanorods and CdS thin films for predominant reflection peak (002) was calculated with Eq. (5) giving 2.2 nm and 18.5 nm , respectively.

EDS analysis of the nanorods (Fig. 2) demonstrated that the organic residues can be removed by several cycles of washing. The product contained about 66 wt% of Cd, 16 wt% of S, 18 wt% of O, along with some impurities like calcium, magnesium and chlorine. The presence of oxygen in CdS nanorods may be due to the insufficient temperature of reaction during their synthesis utilizing CdO. The excess oxygen in the sample might remain in the form of Cd-O or at the interstitial positions (as O^+)

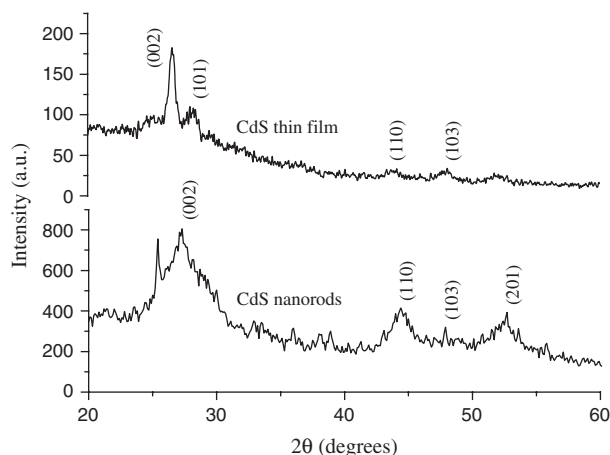


Fig. 1. XRD spectra of CdS: (a) nanorods and (b) nanocrystalline thin film (630 \AA).

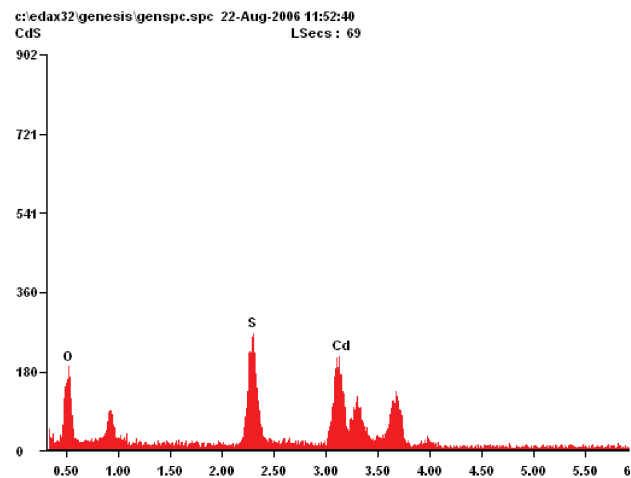
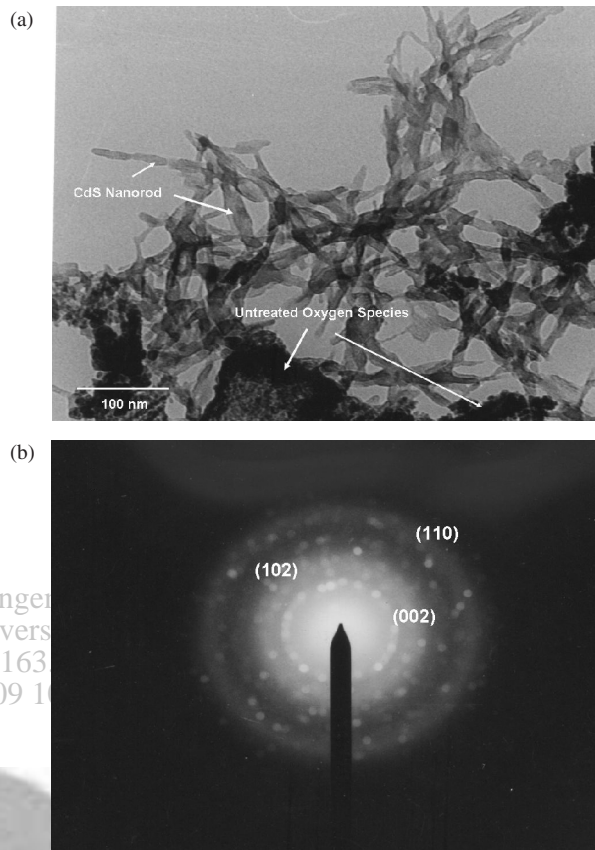
Table I. Structural parameters of CdS nanorods and thin films.

CdS sample	Experimental value		Standard value		Grain size (nm)
	2θ	d (Å)	d (Å)	hkl	
Nanorods	27.3	3.264	3.359	002	2.2
	44.4	2.038	2.070	110	5.9
	52.7	1.735	1.762	112	4.6
Thin films	26.6	3.347	3.359	002	18.5
	28.0	3.175	3.163	101	6.1
	43.7	2.067	2.070	110	6.7
	48.2	1.886	1.899	103	6.7
	52.0	1.755	1.732	201	5.9

in CdS structure. Absence of any diffraction peak related to CdO in the XRD spectrum of the sample clearly indicated that the un-reacted oxygen species took interstitial positions, and might have created sub-surface defects in CdS nanorods.

Formation of rod shaped CdS nanostructures with length in between 8 and 12 nm were observed from the transmission electron microscopy TEM, (Fig. 3(a)). The small dimensions and high surface energy of the nanorods led them to aggregate and form nanorod bundles. From the TEM micrograph we observe that most of the nanorods had elliptical cage linked chain structures, generally observed in MoS₂ nanotubes produced by template method.¹⁵ Such cage linked chain or folded structures depict the flexibility of the nanostructures. Figure 3(b) shows the electron diffraction pattern of an area containing several nanorods, revealing a set of rings and spots due to the random orientation of the nanorods. The rings correspond to the identified (002), (110) and (102) planes of hexagonal CdS phase, which is in agreement with the XRD results.

Figures 4(a–b) shows the two-dimensional atomic force microscopy images of nanocrystalline CdS thin film (630 Å) for two different scan areas, namely 2 μm × 2 μm and 5 μm × 5 μm. The AFM micrographs revealed

**Fig. 2.** A typical EDS spectrum of CdS nanorods.**Fig. 3.** Typical (a) TEM image and (b) electron diffraction pattern of CdS nanorods.

the presence of densely packed nanoparticles on the film surface. From the Figures 4(a and b) the sizes of the grains have been estimated by using Nanoscope instrumental software. The sizes of the grains varied in between 50–100 nm. Moreover, the surface of the films seems to be rough and the root-mean square (rms) surface roughness (R_q) was found to be about 5.39 nm over an 1 μm² area. The grain size estimated from the AFM analysis is much higher than the value estimated from the XRD analysis. This discrepancy is due to the fact that the AFM analysis gives values at the scale of surface microstructure whereas the XRD analysis is considered to be volume effect.¹⁶

The optical absorption spectra of the CdS nanorods and nanocrystalline thin films are shown in the Figures 5(a) and (b), respectively. Excitonic absorption peak for the nanorods and thin films are detected at about 407 nm and 468 nm, respectively, whereas the CdS bulk excitonic absorption band appears at ~515 nm. Such a blue shift of excitonic absorption band can be attributed to the small crystallite size of the samples, and hence the result of quantization effect.

As CdS is a direct band gap semiconductor, its band gap energy can be estimated by means of the $(\alpha h\nu)^2$ versus photon energy ($h\nu$) plot as shown in the inset of Figure 5(b). The band gap was estimated by extrapolating

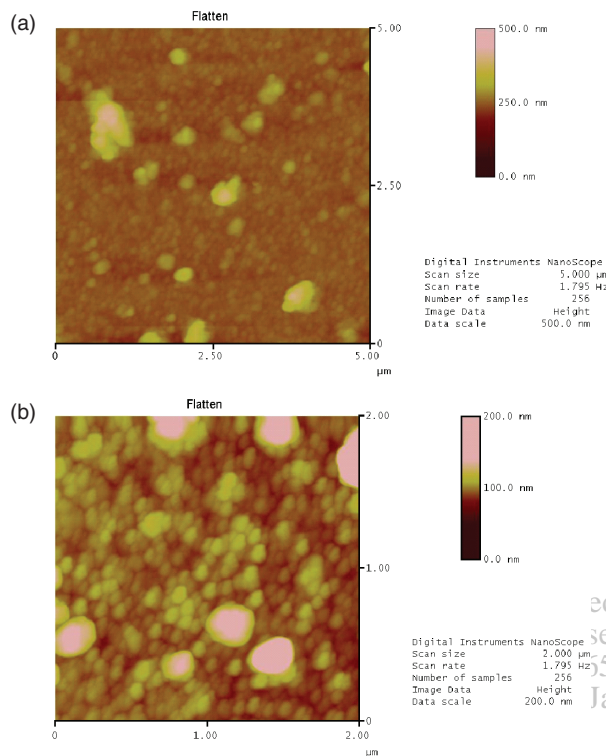


Fig. 4. AFM images of nanocrystalline CdS thin film (630 Å) for different magnification. (a) Two-dimensional micrograph for $5 \times 5 \mu\text{m}^2$ scan area; (b) two-dimensional micrograph for $2 \times 2 \mu\text{m}^2$ scan area.

the linear portion to the energy axis, and was found to be 2.49 eV (± 0.01). The observed bandgap value was slightly higher than its value for bulk CdS (2.42 eV). The observed blue shift of 0.07 eV was due to the quantum confinement effect in CdS films. Similar observations have been reported by Lee et al.¹⁷ and Yu et al.¹⁸ on solution grown CdS nanocrystallites.

3.2. Effect of Reaction Atmosphere

The influence of reaction atmosphere on the particle size and structure of the nanorods were studied by Raman spectroscopy. CdS nanorods were prepared in argon and air atmospheres and their average particle sizes were estimated by the Scherrer formula giving 7 nm and 23 nm, respectively.

Figure 6(a) shows the Raman spectra of CdS nanorods synthesized at different atmospheres. Intensities of the fundamental and first overtone of the LO phonons were used for qualitative understanding of electron–phonon interaction in small particles. Raman spectrum of the CdS nanorods prepared in air ambient displayed a single fundamental band at about 293 cm^{-1} (1LO) and its two overtones at about 585 cm^{-1} (2LO) and $\sim 928 \text{ cm}^{-1}$ (3LO). It was observed that the Raman spectrum contained overtones of weaker intensities than the fundamental,¹⁹ which is in good agreement with the earlier reports

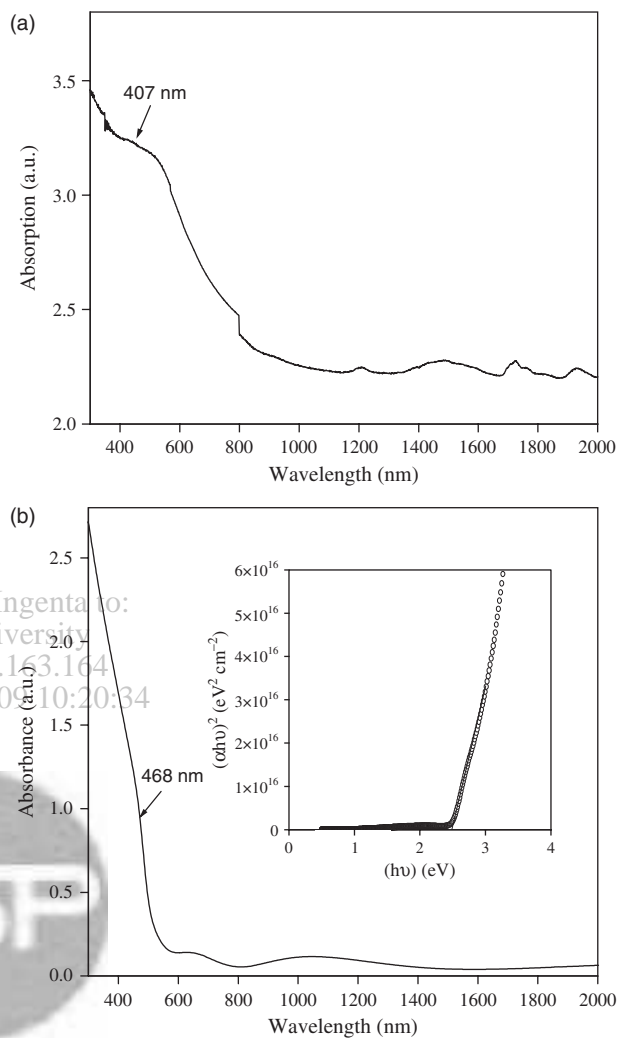


Fig. 5. Optical absorption spectrum of (a) CdS nanorod (b) CdS nanocrystalline thin films (630 Å) [Inset: A plot of $(\alpha h\nu)^2$ vs. photon energy ($h\nu$)].

made by Rajalakshmi et al.²⁰ and Zhang et al.²¹ for CdS nanoparticles. A substantial frequency shift ($\sim 12 \text{ cm}^{-1}$) for the 1LO phonon (293 cm^{-1}) from CdS bulk²² of about 305 cm^{-1} was observed for our CdS nanostructures prepared both in air and argon ambient. The observed Raman shift towards lower frequency might be due to the electron–phonon interaction²³ caused by the reduction of particle size. Figure 6(b) depicts a decrease in the FWHM for the CdS nanorods synthesized in air atmosphere (FWHM: $29.95 \pm 0.69 \text{ cm}^{-1}$) as compared with the nanorods prepared in argon atmosphere (FWHM: $76.52 \pm 2.24 \text{ cm}^{-1}$), which clearly explains the influence of reaction atmosphere during synthesis on particle size. As the crystallite size reduces, there is a clear low-energy shift and a broadening in the Raman scattering peak, which is quite obvious with the description of phonon confinement. Phonon confinement effects may cause the shift in the asymmetrically broaden Raman peak (Fig. 6(b)) when the

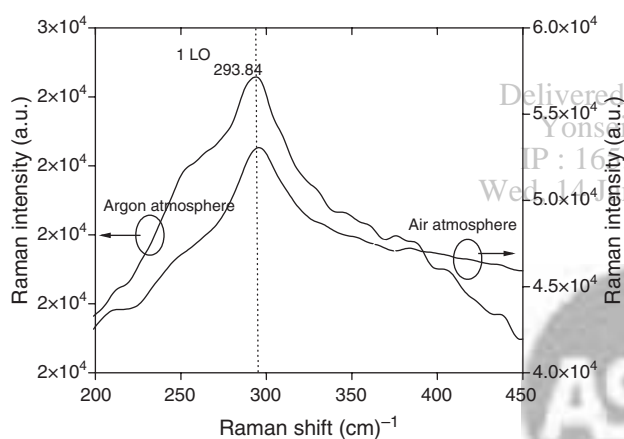
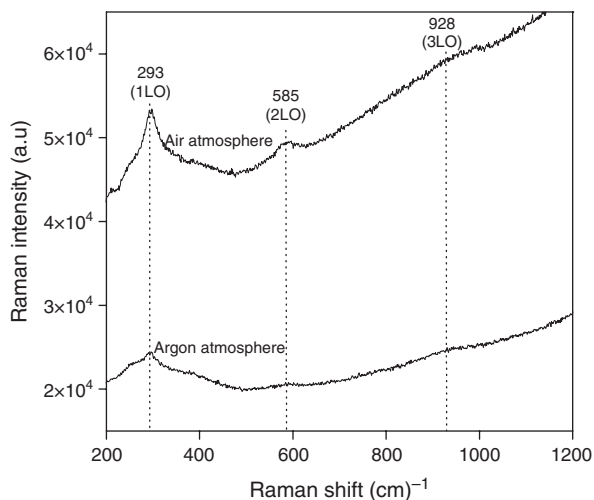


Fig. 6. (a) Raman spectra of CdS nanorods synthesized in argon and air atmospheres. (b) 1LO phonon mode of CdS nanorods prepared in different atmospheres.

crystallite size decreases.^{24, 25} The decrease of the intensity of the overtones (2LO and 3LO) occurs because of the energy of the direct inter-band transition (band gap) moving away from the exciting phonon energy.²⁶ Hence, we concluded that the down-frequency shift and the peak broadening of the Raman spectrum were the results of the quantum confinement or size effects in CdS. From our results, it seems that the argon atmosphere restricted grain growth of the nanorod below some critical size.

3.3. Defect Characterization

The presence of the defects in CdS nanocrystalline thin films were investigated by photoluminescence (PL) spectroscopy. The room temperature PL spectrum of the CdS nanocrystalline thin film is shown in Figure 7. The PL spectrum shows two emission bands around 429 nm (2.9 eV) and 510 nm (2.43 eV). The weak emission at 429 nm arose from the recombination of excitons and shallowly trapped electron-hole pairs,²⁷ which might be due to the presence of unreacted oxygen species as observed in

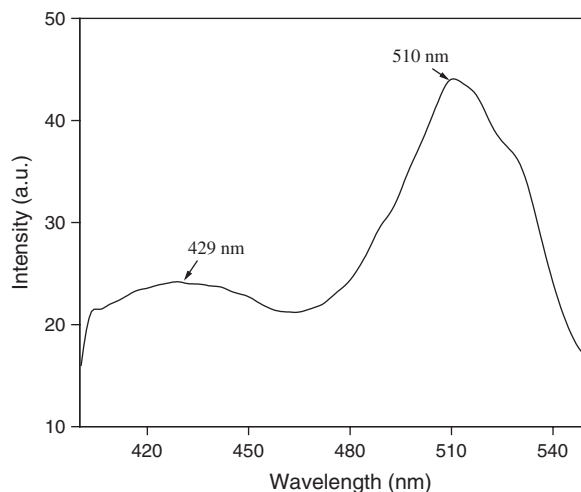


Fig. 7. PL spectrum of the CdS nanorods at room temperature ($\lambda_{ex} = 488$ nm).

the EDS spectrum. The strong emission around 510 nm is in good agreement with the band gap energy of bulk CdS (2.42 eV).²⁸ This could be assigned to the near-band-edge emission of intrinsic nature.

4. CONCLUSIONS

The cadmium sulfide nanorods (~7 nm diameter) were successfully synthesized by organometallic surfactant assisted method. Nanocrystalline thin films were prepared by thermal evaporation of chemically synthesized CdS nanorods. Both the CdS nanorods and CdS thin films exhibit hexagonal phase (Greenockite). Presence of oxygen in our as-grown CdS thin films detected by EDS technique indicates that a further heat treatment of the as-grown CdS nanorods or a higher temperature of reaction is necessary to attain the ideal stoichiometry. The morphology and particle size affect the optical properties of the CdS thin films. Due to small particle size, an intermediate quantum confinement of charge carriers was observed in our nanocrystalline CdS thin films. The reaction atmosphere was found to have strong effects on the particle size control of the nanostructures. Observed down-frequency shift and the peak broadening of the Raman spectrum confirm the quantum confinement effect in CdS nanorods. PL spectra of the CdS nanorods reveal the near band edge emission and the surface recombination defects in them.

Acknowledgments: One of the authors (R. Sathyamoorthy) thanks to University Grants Commission (UGC), New Delhi for the UGC-Research Award-Project No. F-30-1/2004 (SA-II). Authors acknowledge to the Secretary and the Management of Kongunadu Arts and Science College, Coimbatore, India, for their constant encouragement and also for providing necessary facilities to carry out this work.

References and Notes

1. W. Zhang, Z. Liu, C. Zheng, C. Xu, Y. Liu, and G. Wang, *Mater. Lett.* 57, 2755 (2003).
2. M. Law, J. Goldberger, and P. D. Yang, *Annu. Rev. Mater. Res.* 34, 83 (2004); Q. Zhang, F. Huang, and Y. Li, *Colloids Sur., A* 257, 497 (2005).
3. H. Weller, *Angew. Chem. Int. Ed. English* 32, 41 (1993).
4. Y. Wang and N. Herrron, *J. Phys. Chem.* 115, 525 (1991).
5. T. K. Leodidou, W. Caseri, and U. W. Suter, *J. Phys. Chem.* 98, 8992 (1994); H. Zhang, X. Ma, Y. Li, J. Xu, and D. Yang, *Chem. Phys. Lett.* 377, 654 (2003).
6. C. N. R. Rao, A. Govindaraj, F. L. Deopak, N. A. Gunaru, and Manashi Nath, *Appl. Phys. Lett.* 78, 1853 (2001).
7. T. Praveen, V. Parinda, and A. Pushan, *Mater. Lett.* 54, 343 (2002).
8. H. Wang, Y. Zhu, and P. P. Ong, *J. Vac. Sci. Technol., A* 19, 306 (2001).
9. X. C. Wu and Y. R. Tao, *J. Cryst. Growth* 242, 309 (2002).
10. P. K. Ghosh, U. N. Maiti, and K. K. Chattopadhyay, *Mater. Lett.* 60, 2881 (2006).
11. W. Liu, C. Jiu, C. Jin, L. Yao, W. Cai, and X. Li, *J. Cryst. Growth* 269, 304 (2004).
12. J. Zhu, M. Zhou, J. Xu, and X. Liao, *Mater. Lett.* 47, 25 (2001).
13. A. I. Oliva, R. C. Rodriguez, O. S. Canto, V. Sosa, P. Quintana, and J. L. Pena, *Appl. Surf. Sci.* 205, 56 (2003).
14. A. I. Oliva, O. S. Canto, R. C. Rodriguez, and P. Quintana, *Thin Solid Films* 391, 28 (2001).
15. M. Remskar, A. Mrzel, Z. Skraba, A. Jesih, M. Ceh, J. Demsar, P. Stadelmann, F. Levy, and D. Mihailovic, *Science* 292, 479 (2001).
16. K. K. Nanda, S. N. Sarangi, and S. N. Sahu, *Nanostruct. Mater.* 10, 1401 (1998).
17. J. Lee and T. Tsakalakos, *Nanostruct. Mater.* 8, 381 (1997).
18. I. Yu, T. Isobe, and M. Senna, *Mater. Res. Bull.* 30, 975 (1995).
19. N. B. Colthup, L. H. Daly, and S. E. Wiberley, *Introduction to Infrared and Raman Spectroscopy*, Academic Press, New York (1964).
20. M. Rajalakshmi, T. Sakuntala, and A. K. Arora, *J. Phys.: Condens. Matter* 9, 9745 (1997).
21. H. Zhang, D. Yang, X. Ma, Y. Ji, Sh. Li, and D. Que, *Mater. Chem. Phys.* 93, 65 (2005).
22. O. Zelaya-Angel, F. De. Castillo-Alvarado, J. Avendailo-Lopez, A. Escamilla-esquivel, G. Contreras-puente, R. Lozada-Morales, and G. Torres-Delgado, *Solid State Comm.* 104, 161 (1997).
23. V. Sivasubramanian, A. K. Arora, M. Premila, C. S. Sundar, and V. S. Sastry, *Physica E* 31, 93 (2000).
24. R. Rossetti, S. Nakahara, and L. E. Brus, *J. Chem. Phys.* 79, 1086 (1983).
25. A. P. Alivisatos, T. D. Harris, P. J. Carroll, M. L. Steigerwald, and L. E. Brus, *J. Chem. Phys.* 90, 3463 (1989).
26. J. Zhan, X. Yang, D. Wang, S. Li, Y. Xie, Y. Xia, and Y. Qian, *Adv. Mater.* 12, 1348 (2000).
27. Q. Zhao, L. Hou, R. Hunag, and S. Li, *Inorg. Chem. Comm.* 6, 1459 (2003).
28. L. Xu, Y. Su, D. Cai, Y. Chen, and Y. Feng, *Mater. Lett.* 60, 1240 (2006).

Received: 10 January 2007. Accepted: 4 June 2007.

